Polarization-dependent laser action in a two-dimensional random medium

doi: 10.1103/PhysRevE.66.027601

Polarization-dependent laser action in a two-dimensional random medium

Tetsu Ito and Makoto Tomita
Department of Physics, Faculty of Science, Shizuoka University, 836 Ohya Shizuoka, Japan 422-8529
(Received 14 March 2002; published 7 August 2002)

We examined laser action in a two-dimensional amplifying and scattering medium consisting of random array of dye-doped plastic fiber. When the excitation pulse energy was increased, the parallel emission component to the fiber first reached the laser threshold showing spectral collapse, and then further increase in the excitation pulse energy resulted in the subsequent laser action in the perpendicular component. Two-beam spatial-correlation measurement was performed to examine the gain regions. It was found that the size of the gain region is different between the two polarization components. Experimental results on the threshold and the gain region are discussed on the basis of simple rate equations.

DOI: 10.1103/PhysRevE.66.027601 PACS number(s): 42.25.Dd, 42.55.−f, 71.55.Jv

Recently, there have been a lot of studies on laser action in two-dimensional (2D) photonic crystals. There are two ways to realize photonic crystal lasers [1,2]. The first type is to use a localization mode in the band gap [3]. By introducing defect in the crystals, we can pull a state from continuum and make the localized mode, which acts as a cavity with perfectly reflecting walls. The other type is to use the small group velocity intrinsic to the photonic crystal [4]. It has been discussed that the amplification factor is inversely proportional to the group velocity, since propagation modes with the small group velocity stay long time in the crystal, the interaction of light with materials being enhanced.

Periodic structures of crystals may not be necessary to increase the interaction of light with materials in dielectric structures. Light amplification in random media has extensively been studied. The emission spectrum shows spectral collapse and the input-output characteristic curve exhibits a typical behavior similar to a multimode laser [5]. Narrow peaks in the emission spectrum of random laser in ZnO powder have been attracting much attention [6,7]. The measurements have been explained in terms of resonant feedback of the recurrent scattering loops induced by disorder. Although this explanation based on Anderson localization is fascinating, some other effects, such as feedback by the boundary of parallel facets of the hexagonal ZnO microcrystalline [8] or by the surface of the micro sample [9], have also been suggested as the possible mechanisms.

In this paper, we experimentally investigate the random laser action in a 2D medium consisting of random array of dye-doped plastic fiber. In wave propagation, the dimensionality is a crucial parameter. In one- and two-dimensional random systems, arbitrary small disorder will lead to a finite localization length, while in three-dimensional (3D) systems, a certain critical degree of disorder is needed for the localization [10,11]. This means that the coherent feedback due to the recurrent scattering loop would appear easily in 2D systems than 3D systems. Another difference is the polarization effect. In 3D system, two components of polarization are mixed via the scattering process, whereas in 2D system the polarization effects are expected owing to the asymmetric property of the system. We clearly observed the polarization dependent laser threshold and the gain region. Experimental results are discussed on the basis of simple rate equations.

Figure 1 shows the schematic illustration of 2D amplifying and scattering medium consisting of random array of dye-doped nylon fiber. The diameter of the fiber was 15 μm and the refractive index was 1.5. The fiber was first dipped in a methanol solution of kiton red in order to dope dye molecules as the gain medium. The concentration of the dye in the fiber was estimated to be $N=2\times10^{-4}M$, which corresponds to the absorption length, $l_a=490$ μm. The fiber was bundled in air (refractive index is 1.0) to a thickness of 5 mm and a width of 20 mm. The sample without dye appeared opaque and white in color, and no specific laser diffraction pattern was observed. Therefore, we can consider that our micrometer size fibers are in the random alignment and hexagonal-like order is not induced by stacking. The transport mean free path was calculated on the basis of Mie theory [12]. The transport mean fee path l^* is related to the scattering mean free path $l_s=(n_0\sigma_s)^{-1}$ by $l^*=l_s/(1-\langle\cos\theta\rangle)$, where σ_s is the scattering cross section, n_0 is the density of the scatterer, and $\langle\cos\theta\rangle$ is the average angle of scattering of light by a single scattering. The average angle were calculated as $\langle\cos\theta\rangle_{\|}=0.80$ and $\langle\cos\theta\rangle_{\perp}=0.84$ for the parallel and perpendicular emission light in the present sample, respectively. The mean free path of the emission light parallel and perpendicular to the fiber were then calculated as $l_{\|}^*=73$ μm and $l_{\perp}^*=92$ μm, respectively. The excitation light source was the second harmonics of an injec-

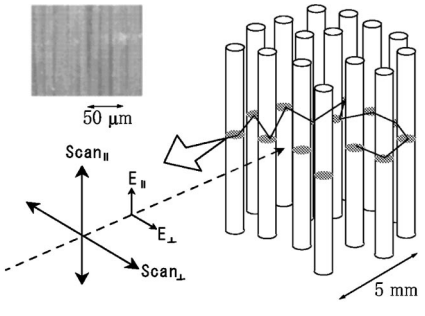

FIG. 1. Schematic illustration of the 2D random sample. $E_{\|}$ and $E_{\perp}$ are the polarization directions of the excitation and the emission light. $\text{Scan}_{\|}$ and $\text{Scan}_{\perp}$ indicate the scanning direction in the two-beam spatial-correlation method. The inset is a photograph of the incident surface of the sample.

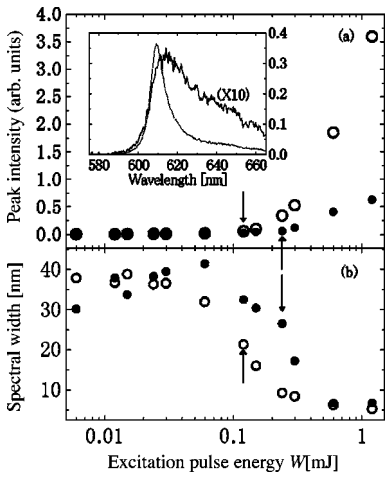

FIG. 2. (a) Semilogarithmic plot of peak intensity, (b) spectral width of the emission as a function of the excitation pulse energy. Open and solid circles represent emission components parallel and perpendicular to the fiber, respectively. Arrows indicate thresholds. The excitation pulse is polarized parallel to the fiber. The inset is the emission spectra of parallel component (dashed line) and perpendicular component (solid line) at the excitation pulse energy, 0.24 mJ.

tion seeded Q-switched Nd^{3+} yttrium-aluminum-garnet (YAG) laser. The wavelength was 532 nm, the pulse duration was 8 ns, and the repetition rate was 1 Hz. The polarization of the excitation pulse was rotated using a $\lambda/2$ wave plate. The spot size of the laser beam on the sample was $w = 100$ μm. The emission light from the incident surface of the sample was collected in a reflection geometry and led to a 25 cm spectrometer through a polarizer, and detected by a charge coupled device camera. The peak wavelength of the emission light from kiton red was 610 nm.

Figures 2(a) and 2(b) show the peak intensity and the spectral width of the emission light as a function of excitation pulse energy W, measured with a single beam. The excitation pulse was polarized parallel to the fiber. Open and solid circles represent emission components parallel and perpendicular to the fiber, respectively. When the excitation pulse energy was increased, the parallel emission component first showed a spectral collapse from the initial width of 35 nm to 5 nm owing to the strong stimulated emission in the sample [5,7] and the peak intensity rapidly grew. As the pulse energy was further increased, the perpendicular component showed a similar behavior. We define the threshold of the laser action as the excitation pulse energy, W_{th}, at which the spectral width becomes half of its initial value. The threshold of parallel and perpendicular emission components were $W_{th\|}^{\|}=0.12$ mJ and $W_{th\perp}^{\|}=0.26$ mJ, respectively, which are indicated by arrows in the Figs. 2(a) and 2(b). We performed similar experiments with the excitation pulse polarized perpendicular to the fiber, and the experimental results on the threshold are summarized in Table I.

The intensity ratio of the parallel to the perpendicular emission components $R=I_{\|}/I_{\perp}$, was calculated from Fig. 2(a) and shown in Fig. 3. When the excitation pulse was polarized parallel to the fiber this ratio is initially $R^{\|}=1.2$.

TABLE I. The polarization dependence of the threshold and the correlation length.

Excitation	Emission	W_{th} (mJ)	L_c^* (μm)
Parallel	Parallel	0.12	760
	Perpendicular	0.26	1090
Perpendicular	Parallel	0.20	
	Perpendicular	0.26	

Above the threshold $W_{th\|}^{\|}$ (0.12 mJ), the ratio increased with increasing excitation pulse energy and approached a constant value of $R^{\|}=5.2$ above the threshold $W_{th\perp}^{\|}$ (0.26 mJ). It is interesting to note that when the excitation pulse was perpendicular to the fiber, the emission component perpendicular to the fiber was stronger, i.e., $R^{\perp}=0.7$ under the weak excitation, whereas above the threshold, the emission parallel to the fiber was enhanced, suggesting the stronger feedback for this polarization component.

We performed a two-beam spatial-correlation measurement to examine the polarization dependence of the size of the gain region [13–15]. In this method, two incident excitation beams are injected onto the sample and the spectral width of the emission is measured as a function of the spatial distance d between two focus spots of the incident beams on the sample. When two beams are spatially overlapped, two excitation pulses work cooperatively to result in the strong spectral collapse, while spatially separated two pulses as, $d \rightarrow \infty$, excite the sample independently. Therefore, the spectral width as a function of d provides direct information on the size of the gain region. Figure 4 shows spectral width $SW(d)$ as a function of the beam separation d. The excitation pulse was polarized parallel to the fiber. The pulse energy was 0.12 mJ and 0.30 mJ for the measurement of parallel and perpendicular emission components, respectively. The triangles show $SW(d)$ for the parallel emission component, where two beams were scanned parallel to the fiber as shown in Fig. 1. Open and solid circles are $SW(d)$ for the parallel

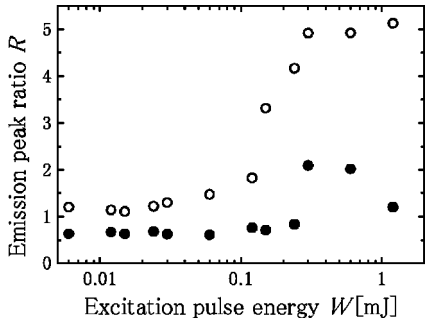

FIG. 3. Semilogarithmic plot of intensity ratio of the parallel emission component to the perpendicular component R. The excitation pulse is polarized parallel (open circles) and perpendicular (solid circles) to the fiber.

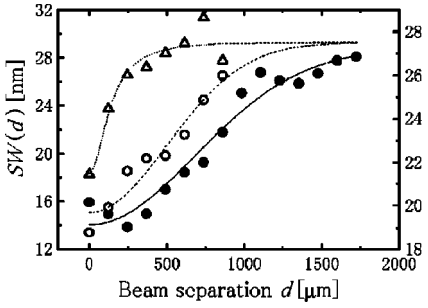

FIG. 4. Spectral width as a function of d in the two-beam spatial-correlation measurement. The emission is polarized parallel (open circles and triangles) and perpendicular (solid circles) to the fiber. The scanning direction is parallel (triangles) and perpendicular (open and solid circles) to the fiber. The left axis is for open circles and triangles, and the right axis is for solid circles.

and perpendicular emission components, respectively, where two beams were scanned perpendicular to the fiber.

We introduce a correlation length L_c as the length that the spectral width becomes $SW(L_c)=\{SW(0)+SW(\infty)\}/2$ and also define a reduced correlation length as $L_c^*=\sqrt{L_c^2-w^2}$ to deconvolute the effect of the finite excitation beam diameter, $w=100$ μm. When the scanning direction was parallel to the fiber, the value $L_c^*=94$ μm obtained from Fig. 4 shows a good correspondence with the beam spot size. This result indicates that the excitation and emission light propagate in the plane normal to the fiber. When the scanning direction was perpendicular to the fiber, $L_{c\|}=760$ μm and $L_{c\perp}=1090$ μm, for the parallel and perpendicular emission components, respectively. The correlation length for the parallel component to the fiber is smaller than that of the perpendicular one. These results are summarized in Table I.

Finally, we performed a time-resolved photoluminescence experiment in order to examine the polarization characteristics of dye molecules in the sample. The excitation light source was the second harmonics of a mode locked Nd^{3+} YAG laser, which provides 80 psec pulses at 532 nm, and the detection system was a synchronous scanning streak camera. The excitation pulse energy was 0.18 nJ and corresponds to the weak excitation limit in Figs. 2 and 3. The time dependence of the photoemission is shown in Fig. 5 on a semi-log scale. Both the parallel and the perpendicular components

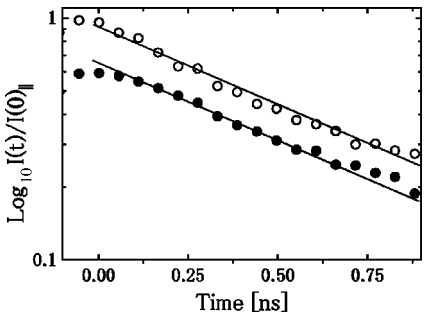

FIG. 5. Time dependence of the emission intensity normalized by the peak intensity $I(0)_{\|}$. The emission is polarized parallel (open circles) and perpendicular (solid circles) to the fiber.

decay exponentially with a time constant of 0.5 nsec. This result means that dye molecules adsorbed inside the fiber are frozen and free from the rotational motion within the time scale examined.

We consider the population of dye molecules in the gain volume on the basis of simple rate equations and discuss experimental results. We note the gain volume as $V_g=L_g^2 w$, where L_g is the size of the gain volume and simply assume that all dye molecules are in excited state in the gain volume, $N_1 \sim N$ [14]. The photon number injected into this volume in unit time is $S \propto W/\hbar\omega$, where $\hbar$ is the Planck constant and ω is the frequency of the excitation light. First, we consider that both the emission and the excitation light are polarized parallel to the fiber. The number of dye molecules that decay via spontaneous and stimulated emissions in the gain volume are represented as $V_g N/\tau$ and $V_g N \Phi_{\|}^{\|} \sigma_s \eta_{\|} c$, respectively, where τ is spontaneous emission lifetime, $\eta_{\|}$ is the projection of the molecular dipole moment to the direction to the fiber, σ_s is the stimulated emission cross section of dye and c is the velocity of light in the medium. The symbol $\Phi_{\|}^{\|}$ represents the density for the emission light, where the upper and the lower notations, $\|$, denote the polarization direction of the excitation and the emission light, respectively. We obtain

$$S=V_g N(1/\tau+\Phi_{\|}^{\|}\sigma_s\eta_{\|}c). \tag{1}$$

For the emission light, it escapes from the gain volume by the diffusion process

$$V_g N(1/\tau+\Phi_{\|}^{\|}\sigma_s\eta_{\|}c)=V_g\Phi_{\|}^{\|}/\tau_d, \tag{2}$$

where $\tau_d=L_g^2/l_{\|}^* c$ is the characteristic time for the light to diffuse out from the gain volume.

Under the weak excitation condition, we can ignore the stimulated emission in Eq. (1), and obtain

$$L_g \propto (S\tau/Nw)^{1/2}. \tag{3}$$

Under the strong excitation condition, the stimulated emission becomes much more important. We can ignore the spontaneous emission term in Eq. (2) and obtain

$$L_{g\|} \propto \left(\frac{l_{\|}^*}{N\sigma_s\eta_{\|}}\right)^{1/2}. \tag{4}$$

We consider that two expressions for the size of the gain region L_g, Eqs. (3) and (4), are equal at the threshold. The threshold is

$$S_{th\|}^{\|}=\frac{l_{\|}^* w}{\sigma_s\tau\eta_{\|}}. \tag{5}$$

In a similar way, we obtain

$$S_{th\perp}^{\|}=\frac{l_{\perp}^* w}{\sigma_s\tau\eta_{\perp}} \tag{6}$$

for the emission light polarized perpendicular to the fiber. From these results, the ratio is

$$\frac{S^{\parallel}_{th\perp}}{S^{\parallel}_{th\parallel}} = \frac{l^*_{\perp}}{l^*_{\parallel}} \frac{\eta_{\parallel}}{\eta_{\perp}}. \tag{7}$$

Similarly, when the excitation pulse is polarized perpendicular to the fiber, we obtain

$$\frac{S^{\perp}_{th\perp}}{S^{\perp}_{th\parallel}} = \frac{l^*_{\perp}}{l^*_{\parallel}} \frac{\eta_{\perp}}{\eta_{\parallel}}. \tag{8}$$

From Eqs. (7) and (8) and the experimental results in Table I, we obtain $l^*_{\parallel}/l^*_{\perp}=0.59$ and $\eta_{\parallel}/\eta_{\perp}=1.3$. This value $l^*_{\parallel}/l^*_{\perp}=0.59$ shows a reasonable agreement with $l^*_{\parallel}/l^*_{\perp}=0.79$, which is obtained from the calculation of Mie theory as described in the experimental description. The slight difference between the experiment and the Mie calculation in $l^*_{\parallel}/l^*_{\perp}$ may arise from simplicity of our model. For example, the parallel emission component may be subject to the total internal reflection at the boundary of sample. This reflection acts as a strong feedback and reduces the laser threshold $S_{th\parallel}$, which also reduces the ratio, $l^*_{\parallel}/l^*_{\perp}$ on the basis of Eqs. (7) and (8) in our model. The value $\eta_{\parallel}/\eta_{\perp}=1.3$ also shows a good agreement with $\eta_{\parallel}/\eta_{\perp}=1.4$ obtained from Fig. 5.

From Eq. (4), the ratio of the gain volume of the perpendicular to the parallel component is

$$\frac{L_{g\perp}}{L_{g\parallel}} = \left(\frac{l^*_{\perp}}{l^*_{\parallel}} \frac{\eta_{\parallel}}{\eta_{\perp}} \right)^{1/2}. \tag{9}$$

Using $l^*_{\parallel}/l^*_{\perp}=0.59$ and $\eta_{\parallel}/\eta_{\perp}=1.3$ obtained above, we get $L_{g\perp}/L_{g\parallel}=1.5$ from Eq. (9). This value is in good agreement with $L_{th\perp}/L_{th\parallel}=1090/760=1.4$ in Table I.

In a 3D system, similar analysis to Eq. (5) leads to the threshold

$$S^{(3)}_{th} = \frac{G^{3/2}_{th} l^{*3/2}}{\sigma_s^{3/2} N^{1/2} \tau}. \tag{10}$$

From Eqs. (5) and (10), the ratio $W^{(2)}_{th}$ to $W^{(3)}_{th}$ is

$$S^{(2)}_{th}/S^{(3)}_{th} = W^{(2)}_{th}/W^{(3)}_{th} = \frac{w}{\eta L^{(3)}_{th}}. \tag{11}$$

Narrow peaks [6,7] in the spectrum were not observed in the present experiment, suggesting that the recurrent loops are not important in the present sample. It is, however, noted that the threshold pulse energy in a real 2D system is smaller than that of 3D system by a factor w/L_{th}, since both the excitation and emission light are confirmed in the plane normal to the fiber.

In conclusion, we observed polarization dependent random laser action in the 2D amplifying and scattering medium. Two polarization components exhibit a behavior similar to a two-mode laser oscillation in an inhomogenously broadened gain medium. When the excitation pulse energy was increased, the parallel component first reached the threshold showing the spectral collapse. Further increase in the excitation pulse energy resulted in the subsequent laser action in the perpendicular component accompanied with the increment of the size of the gain region.

[1] K. Inoue, M. Sasada, J. Kawamata, K. Sakoda, and J.W. Haus, Jpn. J. Appl. Phys. **54**, L157 (1999).

[2] *Optical Properties of Photonic Crystals*, edited by K. Sakoda (Springer, Berlin, 2001).

[3] E. Yablonovitch, T.J. Gmitter, R.D. Meade, A.M. Rappe, K.D. Brommer, and J.D. Joannopoulos, Phys. Rev. Lett. **67**, 3380 (1991).

[4] J.P. Dowling, M. Scalora, M.J. Bloemer, and C.M. Bowden, J. Appl. Phys. **75**, 1896 (1994).

[5] M.N. Lawandy, R.M. Balachandran, A.S.L. Gomes, and E. Sauvain, Nature (London) **368**, 436 (1994).

[6] H. Cao, Y.G. Zhao, S.T. Ho, E.W. Seelig, Q.H. Wang, and R.P.H. Chang, Phys. Rev. Lett. **82**, 2278 (1999).

[7] *Optical Properties of Nanostructured Random Media*, edited by V.M. Shalaev (Springer, Berlin, 2002).

[8] Z.K. Tang, G.K.L. Wong, P. Yu, M. Kawasaki, A. Ohtomo, H. Koinuma, and Y. Segawa, Appl. Phys. Lett. **72**, 3270 (1998).

[9] D. Wiersma, Nature (London) **406**, 132 (2000).

[10] *Scattering and Localization of Classical Waves in Random Media*, edited by P. Sheng (World Scientific, Singapore, 1990).

[11] I. Freund, M. Rosenbluh, R. Berkovits, and M. Kaveh, Phys. Rev. Lett. **61**, 1214 (1988).

[12] *Absorption and Scattering of Light by Small Particles*, edited by C.F. Bohren and D.R. Huffman (Wiley-Interscience, New York, 1983).

[13] K. Totsuka, G. van Soest, T. Ito, A. Lagendijk, and M. Tomita, J. Appl. Phys. **87**, 7623 (2000).

[14] T. Ito and M. Tomita, Phys. Rev. E **63**, 036608 (2001).

[15] T. Ito and M. Tomita, J. Phys. Soc. Jpn. **70**, 2493 (2001).